Simulating walking droplets
18.355 Final Project

Kamal Ndousse

December 16, 2014

1 Introduction

Droplets bouncing on the surface of a vibrating bath of silicone oil can exhibit interesting phenomena, according to Morgan Freeman[1].

Laboratory investigaitons of these hydrodynamical walking droplet systems, prominently including those conducted by Couder, reveal fascinating behavior. This macroscopic system can exhibit phenomena once considered intangible and exclusive to the microscopic world, such as single-particle diffraction[3].

The formulation of an integro-differential equation describing the motion of walking droplets has enabled numerical studies of the statistical behavior of these systems (such as the stability of emergent orbitals in a rotating bath[4]) which may be prohibitively cumbersome in laboratory contexts.

The goal of this project is to develop a framework for computational experiments with walking droplets. Rather than simply predict the paths of simulated droplets, we fully resolve the wave field at every point in time. This approach, while less efficient than alternatives (such as lazy evaluation of the wave field only when needed to calculate the trajectory), permits direct visualization of the full system. Thereby we honor the tradition of art in fluid dynamics.

The code developed in this paper is available at: `https://github.com/kandouss/pilot_wave`.

2 Discretization

The field created by a walking droplet is of the form[2]:

$$h(\mathbf{x},t) = A \sum_{n=-\infty}^{[t/T_F]} J_0\left(K_F \left|\mathbf{x} - \mathbf{x}_p(nT_F)\right|\right) e^{-(t-nT_F)/(MT_F)}, \tag{1}$$

and the position of the droplet is determined by

$$m\ddot{\mathbf{x}_p} + D\dot{\mathbf{x}_p} = -mg\nabla h(\mathbf{x}_p, t). \tag{2}$$

2.1 Field discretization

The field at time $t + T_F$ is

$$\begin{aligned} h(\mathbf{x}, t+T_F) &= A \sum_{n=-\infty}^{[t/T_F]+1} J_0\left(K_F \left|\mathbf{x} - \mathbf{x}_p(nT_F)\right|\right) e^{-(t+T_F-nT_F)/(MT_F)} \\ &= A \sum_{n=-\infty}^{[t/T_F]} J_0\left(K_F \left|\mathbf{x} - \mathbf{x}_p(nT_F)\right|\right) e^{-(t-nT_F)/(MT_F)} e^{-1/M} \\ &+ AJ_0\left(K_F \left|\mathbf{x} - \mathbf{x}_p(t+T_F)\right|\right) \\ h(\mathbf{x}, t+T_F) &= AJ_0\left(K_F \left|\mathbf{x} - \mathbf{x}_p(t+T_F)\right|\right) + e^{-1/M} h(\mathbf{x}, t) \end{aligned} \tag{3}$$

2.2 Discrete particle motion

Similarly we can express the position of the particle at time $t + T_F$ using the centered second-difference approximation for the second derivative

$$\ddot{\mathbf{x}_p}(t) \approx \frac{\mathbf{x}_p(t+T_F) - 2\mathbf{x}_p(t) + \mathbf{x}_p(t-T_F)}{T_F^2} \tag{4}$$

and Sterling's formula for centered differences for the first derivative

$$\dot{\mathbf{x}_p}(t) \approx \frac{\mathbf{x}_p(t+T_F) - \mathbf{x}_p(t-T_F)}{2T_F}. \tag{5}$$

Plugging these into Eq. 2 gives:

$$-g\nabla h(\mathbf{x}_p(t), t) = \frac{\mathbf{x}_p(t+T_F) - 2\mathbf{x}_p(t) + \mathbf{x}_p(t-T_F)}{T_F^2} + \frac{D}{m}\frac{\mathbf{x}_p(t+T_F) - \mathbf{x}_p(t-T_F)}{2T_F}. \tag{6}$$

Solving for $\mathbf{x}_p(t + T_F)$, we find:

$$\mathbf{x}_p(t+T_F) = \left(\frac{4m}{2m+DT_F}\right)\mathbf{x}_p(t) + \left(\frac{DT_F - 2m}{DT_F + 2m}\right)\mathbf{x}_p(t-T_F) - \left(\frac{2T_F^2 g}{DT_f + 2m}\right)\nabla h(\mathbf{x}_p(t), t). \tag{7}$$

2.3 Nondimensionalization

The expressions giving the discrete time evolution of the field (Eq. 3) and droplet (Eq. 7) can be simplified by introducing the following non-dimensional variables:

$$Q \equiv \frac{DT_F}{2M}, \text{ and} \tag{8}$$

$$S \equiv T_F^2 g A K_F. \tag{9}$$

Q encapsulates properties which could vary between droplets on a single field (in particular, mass and drag), and S accounts for general properties of the wave field (amplitide of bounces, gravitational force, faraday wave number).

In terms of these parameters, Eqs. 3 and 7 become:

$$h(\mathbf{x}, t + T_F) = SJ_0\left(K_F \left|\mathbf{x} - \mathbf{x}_p(t + T_F)\right|\right) + e^{-1/M} h(\mathbf{x}, t) \tag{10}$$

$$\mathbf{x}_p(t + T_F) = \left(\frac{2}{Q+1}\right)\mathbf{x}_p(t) + \left(\frac{Q-1}{Q+1}\right)\mathbf{x}_p(t - T_F) - \left(\frac{1}{K_F(Q+1)}\right)\nabla h(\mathbf{x}_p(t), t) \tag{11}$$

Finally, we switch to more suggestive notation for discrete numerical computation by defining:

$$\mathbf{x}_p[n] = \mathbf{x}_p(nT_F), \text{ and} \tag{12}$$

$$h_n[\mathbf{x}] = h(\mathbf{x}, nT_F) \tag{13}$$

We then have:

$$h_{n+1}[\mathbf{x}] = e^{-1/M} h_n[\mathbf{x}] + SJ_0(|\mathbf{x} - \mathbf{x}_p[n+1]|), \text{ with} \tag{14}$$

$$x_p[n+1] = \left(\frac{2}{Q+1}\right)\mathbf{x}_p[n] + \left(\frac{Q-1}{Q+1}\right)\mathbf{x}_p[n-1] - \frac{1}{Q+1}\nabla h_n[x]. \tag{15}$$

We assume that T_F and $1/K_F$ are very small. In order that this model be consistent with the physical vibrating bath system, the length and time scale of the vertical motion (e.g. T_F and K_F must be much smaller than those of the horizontal translational motion. [Oza, bush, ...] also make a very similar assumption in the derivation of the time-averaged integral equation of motion for a droplet.

3 Implimentation

The simulation described here uses Eq. 15 to evolve the spatial trajectories of any number of droplets, while using Eq. 14 to describe the time-averaged shape of the wave field.[1]

3.1 Data structures

The wave field at time $t + nT_F$ is represented by a two-dimensional array of double-precision floating-point values, $h_n[\mathbf{x}]$. The grid spacing is $1/K_F$. The state of each droplet is determined by two coordinates: its current position, and its position at the previous time-step.

The wave field is calculated at every point in the grid at every time step. This approach was chosen (instead of, for example, computing the values of the Bessel functions only where necessary to calculate the wave field gradient at a droplet position) for ease of implementation and visualization.

[1] The code described here, along with source for this documentation and a program to make animations of simulations, is available at `https://github.com/kandouss/pilot_wave`.

3.2 Stability

It is clear that calculation of the wave field gradient is a big source of error. In particular, the field is only defined on grid points, but the droplet positions are nominally represented by floating-point numbers. Estimating the gradient of the field at an arbitrary point by the gradient at the nearest grid point seems to introduce too much error. The gradient is instead calculated using a weighted average of the gradients at the four nearest grid points.

4 Potentials

Suppose the motion of the drop is influenced by a potential $U(\mathbf{x}-\mathbf{x}_0)$. For simplicity, suppose that the wave field is not altered by the presence of this potential.

The equation governing the motion of the droplet (Eq. 2) becomes:

$$m\ddot{\mathbf{x}_p} + D\dot{\mathbf{x}_p} = -mg\nabla h(\mathbf{x}_p, t) - \nabla.U \tag{16}$$

The discretized motion of the droplet under the influence of U is then given by:

$$x_p[n+1] = \left(\frac{2}{Q+1}\right)\mathbf{x}_p[n] + \left(\frac{Q-1}{Q+1}\right)\mathbf{x}_p[n-1] - \frac{1}{Q+1}(\tilde{F}(\mathbf{x}_p[n])) - \frac{1}{Q+1}\nabla h_n[x], \tag{17}$$

where $\tilde{F}$ is proportional to the forcing of the droplet:

$$\tilde{F}(\mathbf{x}) \equiv \frac{1}{(Q+1)}\frac{T_F^2}{m}\nabla U(\mathbf{x}-\mathbf{x}_0). \tag{18}$$

4.1 Spring potential

If the droplet is in a spring potential centered at $\mathbf{x}_0$, then

$$U = \frac{1}{2}m\omega^2\left|\mathbf{x}-\mathbf{x}_0\right|^2 \tag{19}$$

$$\tilde{F}(\mathbf{x}) = \frac{T_F^2\omega^2}{Q+1}(\mathbf{x}-\mathbf{x}_0) \tag{20}$$

$$= \frac{\Omega^2}{Q+1}(\mathbf{x}-\mathbf{x}_0), \tag{21}$$

where $\Omega = T_F\omega$; and the discrete drop motion equation (Eq. 17) becomes

$$x_p[n+1] = \left(\frac{2}{Q+1}\right)\mathbf{x}_p[n] + \left(\frac{Q-1}{Q+1}\right)\mathbf{x}_p[n-1] - \frac{\Omega^2}{Q+1}(\mathbf{x}_p[n]-\mathbf{x}_0) - \frac{1}{Q+1}\nabla h_n[\mathbf{x}] \tag{22}$$

4.2 Central Coulomb potential

If the droplet is in a central Coulomb potential, then

$$U = \frac{\kappa}{|\mathbf{x}|} \tag{23}$$

$$\tilde{F}(\mathbf{x}) = -\kappa \frac{\mathbf{x}}{|\mathbf{x}|^3} \tag{24}$$

5 Many Interacting Particles

Even in the absence of an external potential, multiple droplets bouncing on the same surface will interact. Of the simple simulations performed in the course of this investigation, the behavior of large groups of particles $(25 - 100)$ proved to be the most interesting.

Figs. 5, 5 and 5 show the stable configurations of many very close droplets. Specifically, the average distance between the particles is much less than the wavelength of the wave field variations. The most interesting part of these images (as made clear by the videos linked in the captions) is the variation in density of the distributions of particles. There is clearly a local minimum in the wave field at every dot. We intuitively expect high-density regions to correspond to areas where the wave field is lower.

6 Next steps

The most obvious omission from this project is boundary conditions – in the presence of a wall, interactions between a droplet and its reflected wave field give rise to even more interesting phenomena. Unfortunately the simulation framework developed above doesn't have a natural way of including wave reflections, and there isn't an obvious way to compute the wave field including reflections without detriment to simulation performance. However, I am interested in modifying the programs to replicate the more fascinating walking droplet phenomena, including self-interference.

I plan to simulate a significantly larger number of droplets, and to investigate the correspondence between droplet density and the underlying wave field. I am also interested in looking for analytical approaches to study the behavior of a "continuum" of walkers.

References

[1] Through the wormhole: Wave/particle duality via silicon droplets.

[2] John W. M. Bush. Pilot-wave hydrodynamics. *Reviews in Advance*, preprint, 2015.

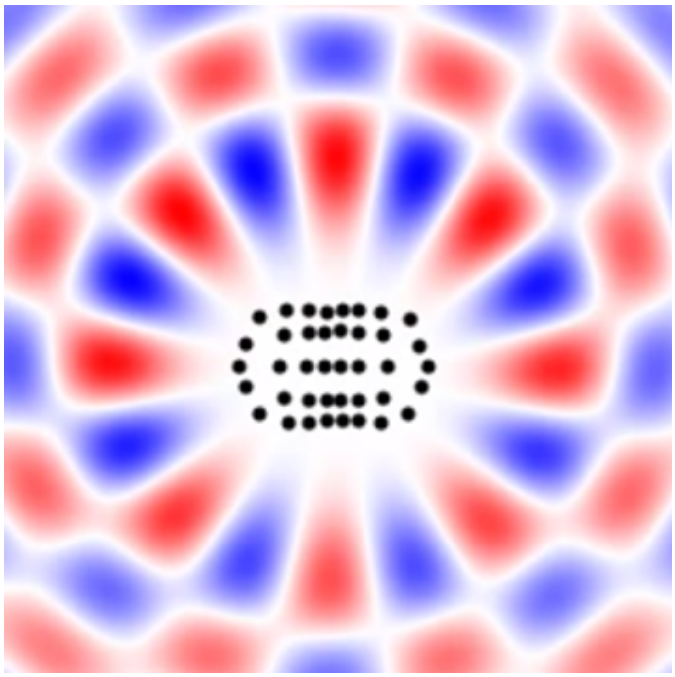

Figure 1: Steady-state late-time image of wave field from 40 walkers. Positions marked by black dots are approximate. Full video available at `http://youtu.be/UnI8ZO_F9l8`.

[3] Y. Couder and E. Fort. Single particle diffraction and interference at a macroscopic scale. *Physical Review Letters*, 97(154101), 2006.

[4] Anand U. Oza, Oistein Wind-Willassen, Daniel M. Harris, Rodolfo R. Rosales, and John W. Bush. Pilot-wave hydrodynamics in a rotating frame: Exotic orbits. *Physics of Fluids*, 26(082101), 2014.

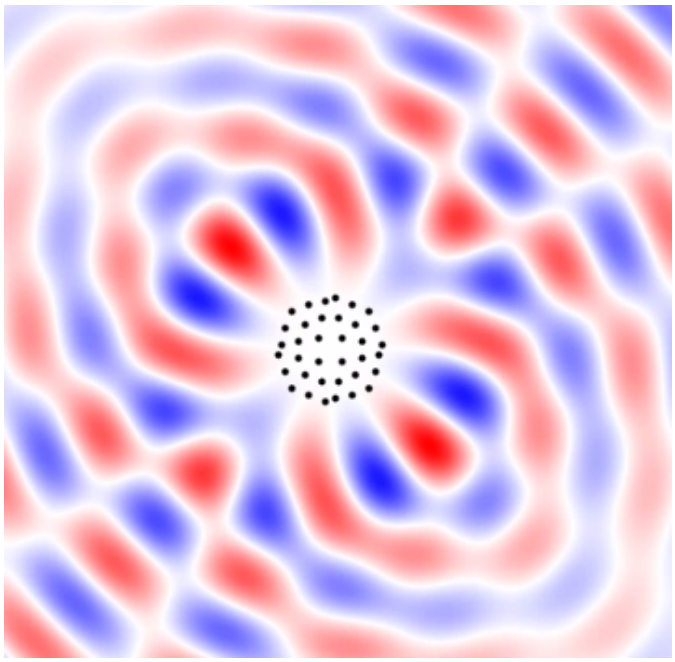

Figure 2: Steady-state late-time image of wave field from 25 walkers. Positions marked by black dots are approximate. Full video available at `http://youtu.be/ArzMcxQf1Gk`.

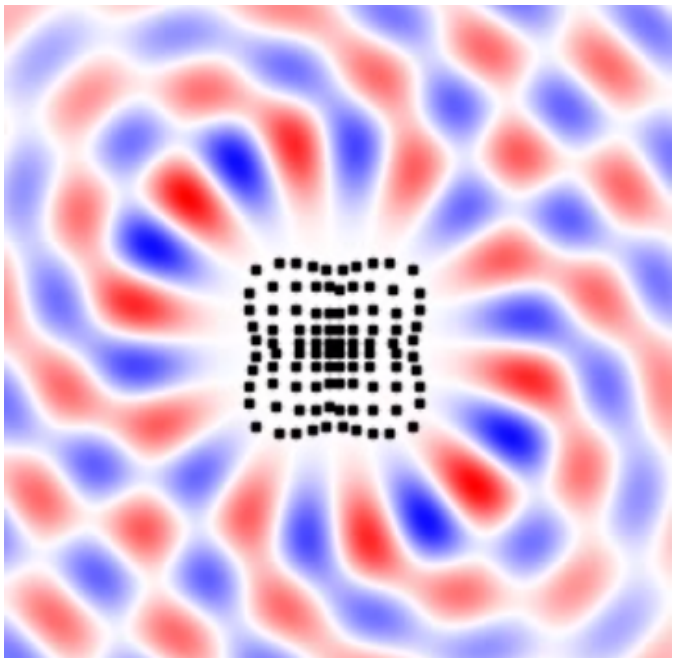

Figure 3: Steady-state late-time image of wave field from 100 walkers. Positions marked by black dots are approximate. Full video available at `http://youtu.be/JOheG5o-1aQ`.